# THREE KINDS OF HEAT TRANSFER AUGMENTATION

## IN PERFORATED SURFACES

Wen-Jei Yang
Department of Mechanical Engineering
University of Michigan
Ann Arbor, Michigan  48109

(Communicated by J.P. Hartnett and W.J. Minkowycz)

ABSTRACT
      Heat exchanger cores, each consisting of a number of single or com-
      posite perforated plates separated by wooden spacers to form parallel
      flow channels, were tested in a subsonic wind tunnel.  Three distinct
      types of augmentation in the heat transfer and friction loss perform-
      ance have been identified:  the transition-turbulent flow enhancement,
      the "second" laminar flow enhancement and the laminar flow enhancement.
      The first kind is observed to occur in the transition and turbulent
      flow regimes on low porosity surfaces [1].  The second type is detected
      in the "second" laminar flow regime on high porosity surfaces [2].
      The present study has revealed the existence of the third pattern
      which occurs over the entire laminar flow region on low-porosity com-
      posite surfaces consisting of a short upstream section for producing
      vortices and a main section for heat transfer.  An attempt is made to
      explain the enhancement mechanisms.

## Introduction

    The need for small size, lightweight, high performance heat exchangers
in all varieties of powered vehicles from automobiles to spacecraft, as well
as a multitude of other applications, has motivated the development of several
kinds of extended surfaces such as plain fin, louvered fin, offset fin and
perforated fin.  While the perforated surface has heat transfer and friction
loss performance comparable to the louvered or offset-plate fin surface, its
compactness is literally unlimited by geometry.

    A series of studies have been conducted for determining the performance
of perforated heat transfer surfaces:  Liang et al [1] have concluded that
for low porosities up to about 20 percent, perforations produce a significant

increase in heat transfer and friction performance only in the transition and
turbulent flow regimes accompanied by flow induced noise and vibration. For
optimum performance, perforations must have the slot-width-to-plate-thickness
ratio $(d_s/t)$ of about 2.0 and the plate-spacing-to-plate thickness ratio $(b/t)$
must be about 2.0 to 3.0. With the motivation of developing perforated sur-
faces of high performance but free of flow-induced noise and vibration, Lee
et al [2] have extended the study to high porosity surfaces of up to 39.7 per-
cent. A substantial augmentation in heat transfer and friction loss is achieved
in the "second" laminar flow regime preceeding the occurrence of flow transi-
tion.

In the present study, a short fibre-glass perforated plate is placed up-
stream from each aluminum perforated plate, forming a composite heat transfer
surface. The upstream plates are to induce periodic shedding of vortices which
travel downstream to disturb both the boundary layers formed on the succeeding
aluminum plates and the main stream between two adjacent plates. Both the
heat transfer and friction loss performance of the composite surfaces are
studied in a subsonic wind tunnel. Results are compared with those of non-
perforated and perforated surfaces obtained in the previous studies [1-3].
An attempt is made to explain the enhancement mechanisms.

<u>Experimental Apparatus and Procedure</u>

Figure 1 shows a schematic diagram of the test facility designed for
transient testing. It consists of a heat exchanger test core situated in a
subsonic wind tunnel.

The test core consists of two sections: an inducing section situated
upstream and a main section that follows, see Fig. 2. The upstream section
was composed of a number of 0.0813 cm (thickness) x 19.1 cm (width) x 15.24 cm
(length in flow direction) fibre-glass (Sythane G 10 with specific gravity
of 1.90) plates, while the main section consisted of the same number of 61 cm
long aluminum (with specific gravity of 2.78) plates of identical thickness
and width. Wooden spacers were used to separate the fibre-glass and aluminum
plates which were lined up to form parallel flow channels. All plates in each
section were identically perforated with slotted holes of a staggered arrange-
ment (see Fig. 3). The number and size of the slotted holes were varied to
give different values of the surface porosity $\sigma_s$, while the thickness of the
wood slabs determined the frontal porosity $\sigma_F$. The total number of the plates
and slabs determines the frontal area of the test core which was 15.2 cm wide

(W), 15.2 cm high and 76.2 cm long in the flow direction (including 15.2 cm of the inducing section and 61 cm of the main section).

The test core was installed in the test section of the wind tunnel. Two pitot tubes, one upstream and the other downstream of the test core, were employed to determine the pressure differences with the aid of a CGS 523-1 Barocel differential pressure transducer and a CGS 1023 electronic manometer. The inlet air temperature was measured by three thermocouples upstream, while the average exit air temperature was determined by a thermocouple grid consisting of 20 thermocouples joined in series. An L & N 8662 precision potentiometer was used to read steady-state temperatures, while transient temperature measurement was recorded on a Honeywell model 1046 visicorder.

A heating screen consisting of a layer of 100x100 mesh, 0.00787 cm diameter nichrome wire screen was installed at the inlet of the test section. Electric current was supplied through a knife switch by a variable current a-c welder.

For testing, the air temperatures upstream and downstream of the test core and pressure differences were taken at each desired air velocity. A step power input from the a-c welder, enough to raise the temperature of the incoming air by about 15 °C, was applied to the heating screen by closing the snife switch. The transient temperature of the air leaving the test core was continuously recorded on the visicorder. Details of the experimental apparatus and procedure are available in reference 1.

## Test Results and Discussion

The heat transfer and friction loss performance of the perforated surfaces were presented in terms of the heat transfer factor j and the friction factor f, respectively. All j and f data were reduced by treating the test plates as nonperforated ones. For heat transfer calculations, all physical properties of air were evaluated at the mean temperature of the air during the transient.

The flow velocity entering the core is evaluated using the Bernoulli equation, while the flow velocity inside the core is calculated based on continuity. The Reynolds number is defined on the basis of the hydraulic diameter of the flow channels in the core as $Re = D_h G/\mu$ where $D_h = 2Wb/(W+b)$ for the present system. The friction factor f is determined from the static pressure drop across the test core corrected for entrance and exit losses:

$$f = \frac{D_h}{4L} \left[ \frac{2g_c \rho \Delta P}{G^2} - (K_c + K_e) \right] \tag{1}$$

The heat transfer coefficient h was determined by a modified single-blow transient test technique described in references 3 and 4. The total mass of the aluminum plates (in the main section) was used as the mass of the test core while h was determined for the surface area of these plates exposed to the air flow. The heat transfer factor j was defined as

$$j = \gamma h Pr^{2/3} / (G\, C_a) \tag{2}$$

where $\gamma$ is a ratio of heat transfer area of a perforated aluminum plate to that of a nonperforated one with the same physical dimension:

$$\gamma = 1 - \sigma_s + \frac{2\pi + (W_s/d_s - 1)}{(P_\ell/d_s)(W_s/t + a/t)} \tag{3}$$

Several composite cores were fabricated and tested. Their geometric properties are listed in Table 1. Representative results are presented in Figs. 4 and 5. All test cores have the same frontal porosity of 0.872. The main cores S2-1 and S4-31 were tested in references 1 and 3 together with the nonperforated core NP-1 of identical flow length (L = 0.61 m) and frontal porosity. The composite cores C2-S4-31, C2-S2-1 and C1-S2-1 consist of the inducing section C1 or C2 and the main section S4-31 or S2-1.

Three distinct flow regimes can be identified in the experimental results of all cores, single as well as composite ones. The laminar flow regime is evidenced by a continuous decrease in f and j with increasing Re. The transition flow regime is featured by an upturn of f and j as Re continues to increase beyond the laminar value. This regime prevails until a value of Re is attained beyond which the values of f and j begin to fall with a further increase in Re, and the fluid flow is now in the turbulent flow regime. Both Figs. 4 and 5 indicate that perforations (cores S4-31 and S2-1) induce earlier (compared with the NP-1 core) transition from laminar to turbulent flow and they produce significant increase in f and j factors in the transition and turbulent flow regimes. Flow visualization studies [5,6] have revealed the alternative shedding of vortices from the upstream edges of the perforated slots. When travelling downstream of the slot, the vortices "eat" into the boundary layers, resulting in an appreciable increase in f and j.

For the high porosity surfaces, Lee et al [2] have disclosed the existence of a critical Raynolds number $Re_0$ beyond which perforations cause the heat transfer and flow friction performance to deviate from those of the nonper-

forated plate in the laminar flow regime (solid lines) and create a "second"
laminar-flow regime (broken lines), see Fig. 6. It is observed that for Re
less than $Re_0$ (corresponding to an intersection of solid and broken lines),
perforations exert no effect on the transport phenomena. In other words,
f or j coincides with that of a nonperforated plate. However, when Re ex-
ceeds $Re_0$, for example about 1500 in case of $\sigma_s = 0.177$, the test data follow
a straight (broken) line of a different slope. The flow in the core is still
in laminar fashion unitl a transition Reynolds number (about 3000 for $\sigma_s = 0.177$)
is reached. The existence of this "second" laminar flow regime becomes more
prominent, beginning at a lower value of $Re_0$ and extending over a broader
range of Re, as the plate porosity is increased as illustrated in Fig. 6. In
reference to the conclusion obtained by Sarohia [7] from his study on the
cavity flow, Lee et al [2] have theorized that the oscillation of free shear
layer in the perforation causes periodic shedding of vortices at the down-
stream edge when Re exceeds $Re_0$. These vortices then interrupt the laminar
boundary layer that is developed on the plate surface immediately downstream
from the hole, resulting in the "second" laminar flow enhancement.

In the present study, the inducing section of the composite cores con-
sist of perforated fibre-glass plates, whose thermal diffusivity is two-orders-
of-magnitude lower than that of the aluminum plates in the main section.
Therefore, the inducing section contributes only to the magnitude of f but
affects j very little on the composite surfaces. It is seen in Figs. 4 and 5
that both f and j are significantly increased in the entire laminar flow re-
gime in the presence of an inducing section. While the flow transition is
delayed, the upstream section does not affect f and j in the turbulent flow
regime. This particular feature is very desirable and useful in application
to the plate-fin type heat exchanger which is mostly operated within this Re
range. It is believed that the transport enhancement in the laminar flow re-
gime is due to the disturbing of the bulk flow and the interruption of the
laminar boundary layers in the main section by the vortices that are period-
ically generated from the perforations in the upstream inducing section.

## Concluding Remarks

It is important to bear in mind that only those perforated plates under
certain restrictions can produce appreciable transport augmentation: for
optimum performance, perforations must have $d_s/t$ of about 2.0 and the perfor-
ated plates must be arranged at $b/t$ of around 2.0 to 3.0. Within these con-
finements, three distinct types of transport enhancement are observed in the

flows over perforated surfaces:  the transition-turbulent flow enhancement
for low-porosity plates, the "second" laminar flow enhancement for high-
porosity plates and the laminar flow enhancement for composite plates.  The
third type is most desirable with the second kind as the next best, since
compact heat exchangers are mostly operated in the laminar flow regime.  The
first pattern enhancement is the least desirable as it is accompanied by
flow-induced noise and vibration.  The mechanisms of the second and third
type enhancement have yet to be investigated in the future through flow vis-
ualization study.

## Nomenclature

| | |
|---|---|
| a | slot spacing, cm |
| b | plate spacing, cm |
| $C_a$ | specific heat of air at constant pressure, J/(kg · K) |
| $d_s$ | slot width, cm |
| $D_h$ | hydraulic diameter, m |
| f | Fanning friction factor |
| $g_c$ | conversion factor, 1.0 (kg · m)/(N · S$^2$) |
| G | mass velocity, kg/(m$^2$ · S) |
| h | heat transfer coefficient, W/(m$^2$ · K) |
| j | heat transfer factor as defined by eq. (2) |
| $K_c$, $K_e$ | entrance and exit pressure loss coefficients in eq. (1) |
| L | length of test core in flow direction, m |
| $\Delta P$ | static pressure drop across test core, N/m$^2$ |
| $P_\ell$ | longitudinal pitch, cm |
| Pr | Prandtl number |
| $P_t$ | transverse pitch, cm |
| Re | Reynolds number; Re$_0$, a critical value for onset of second laminar flow regime due to perforation |
| t | plate thickness, cm |
| W | width of test core, cm |
| $W_s$ | width of slot, cm |
| $\gamma$ | heat transfer area ratio defined by eq. (3) |
| $\mu$ | absolute viscosity, N·S/m$^2$ |
| $\rho$ | density of air, kg/m$^3$ |
| $\sigma_F$ | frontal porosity, 1/(1 + t/b) |
| $\sigma_s$ | plate porosity, $\dfrac{\pi/4 + (W_s/d_s - 1)}{(P_\ell/d_s)(a/d_s + W_s/d_s)}$ |

## References

1.  Liang, C.Y. and Wen-Jei Yang, "Heat Transfer and Friction Loss Perform-
    ance of Perforated Heat Exchanger Surfaces," J. Heat Transfer, Trans.
    ASME, Ser. C, 97, 9 (1975).

2.  Lee, C.P. and Wen-Jei Yang, "Augmentation of Convective Heat Transfer
    from High-Porosity Perforated Surfaces," to be presented at the Sixth
    International Heat Transfer Conference, August 1978, Toronto.

3.  Liang, C.Y., "Heat Transfer, Flow Friction, Noise and Vibration Studies
    of Perforated Surfaces," Ph.D. Thesis, Mechanical Engineering Depart-
    ment, University of Michigan, Ann Arbor, Michigan, 1975.

4.  Liang, C.Y. and Wen-Jei Yang, "Modified Single-Blow Technique for Per-
    formance Evaluation on Heat Transfer Surfaces," J. Heat Transfer, Trans.
    ASME, 97, 16 (1975).

5.  Liang, C.Y., C.P. Lee and Wen-Jei Yang, "Visualization of Fluid Flow Past
    Perforated Surfaces," Proceedings of 4th Japanese Symposium on Flow Vis-
    ualization, July 15-16, 1975, Tokyo, pp. 69-73.

6.  Loehrke, R.I., Roadman, R.E. and Read, G.W., "Low Reynolds Number Flow
    in Plate Wakes," ASME Paper No. 76-WA/HT-30 presented at ASME Winter
    Annual Meeting, Dec. 5, 1976, New York.

7.  Sarohia, V., "Experimental and Analytical Investigation of Oscillations
    in Flows Over Cavities," Ph.D. Thesis, Aeronautical Engineering Depart-
    ment, California Institute of Technology, Pasadena, Calif., 1975.
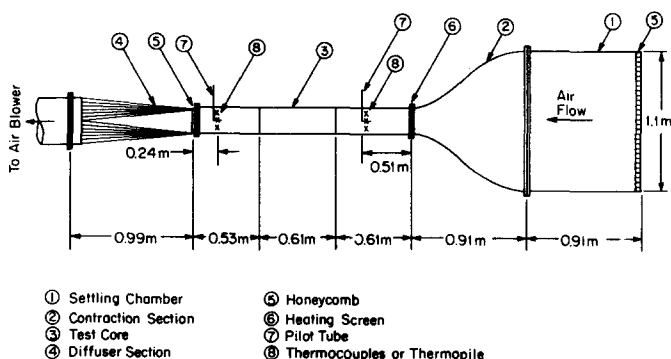
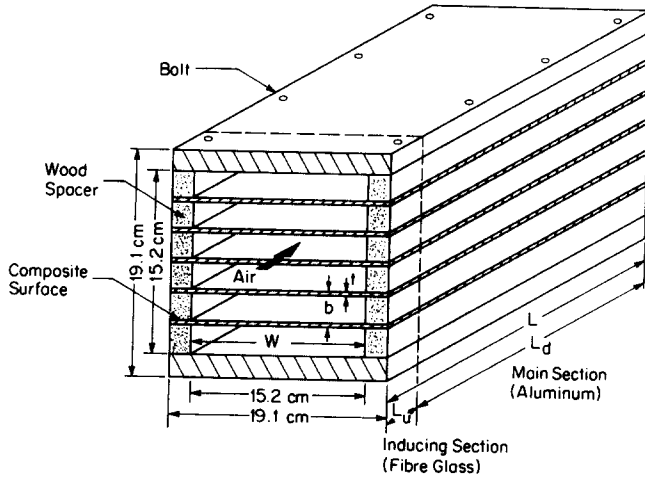FIG. 1    A schematic diagram of test apparatus
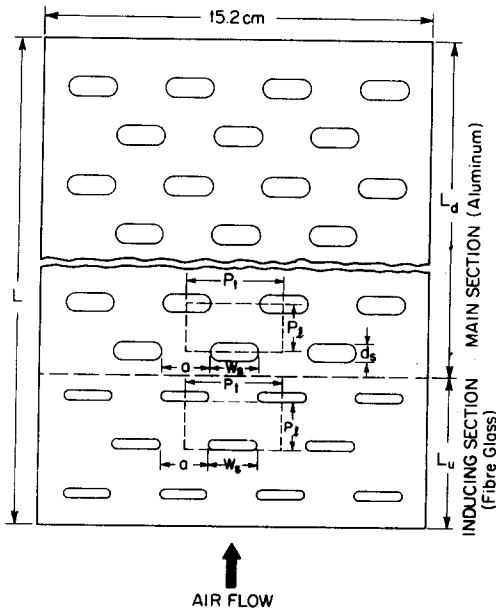
FIG. 2     Test Core



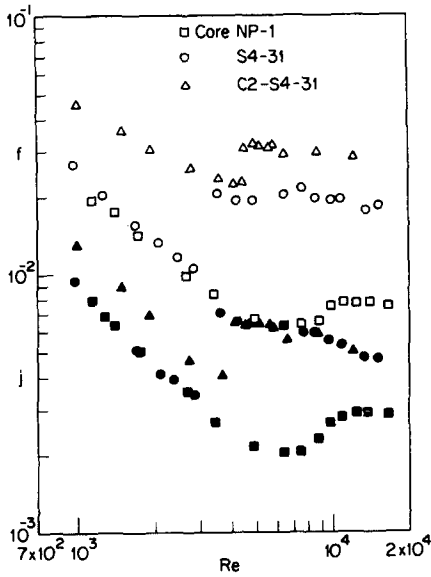FIG. 3     Perforation pattern of composite plate

FIG. 4   Transition-turbulent flow en-
hancement and laminar flow en-
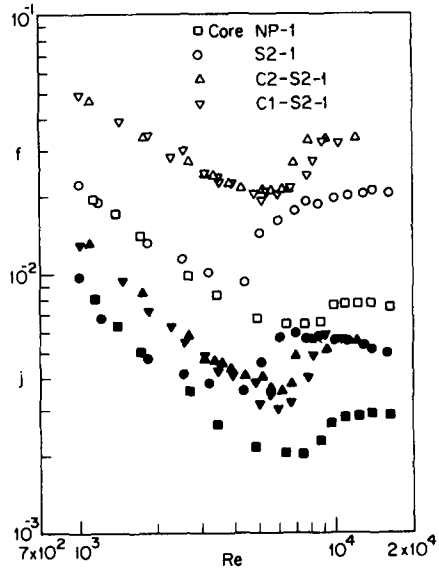hancement.

FIG. 5   Effect of inducing section on
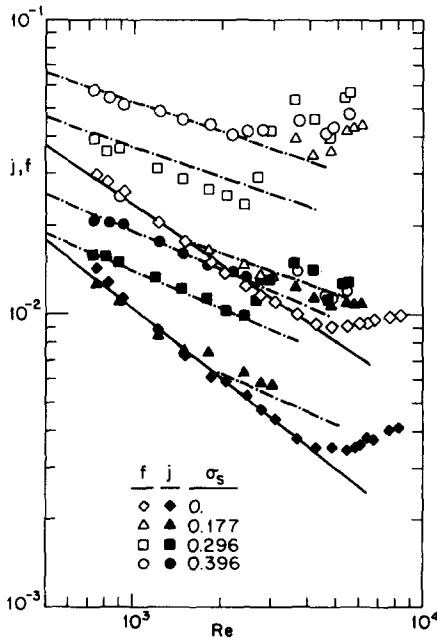laminar flow enhancement



FIG. 6   "Second" laminar flow enhancement

TABLE 1

Geometric Parameters of Composite Cores

|  | Main Section | | Inducing Section | |
|---|---|---|---|---|
|  | S2-1 | S4-31 | C1 | C2 |
| L, m | 0.61 | 0.61 | 0.152 | 0.152 |
| $d_s$, cm | 0.159 | 0.318 | 0.159 | 0.159 |
| $W_s$, cm | 1.27 | 1.27 | 1.27 | 1.27 |
| a, cm | 1.27 | 1.27 | 1.27 | 1.27 |
| $P_t$, cm | 2.54 | 2.54 | 2.54 | 2.54 |
| $P_\ell$, cm | 0.605 | 1.17 | 0.635 | 0.318 |
| $\sigma_s$ | 0.128 | 0.129 | 0.122 | 0.243 |

t = 0.0813 cm,   W = 15.2 cm,   height of test core = 15.2 cm,

b = 0.555 cm,   $\sigma_F$ = 0.872